WEP Warwick Evans Publishing

International Journal of Natural Resources and Environmental Studies

ISSN: 3006-2012 (Print), ISSN: 3006-0834 (Online) | Volume 5, Number 3, Year 2025
DOI: https://doi.org/10.62051/ijnres.v5n3.03
Journal homepage: https://wepub.org/index.php/IJNRES/index

Study on the Physical Properties of Deep Coalbed Methane Reservoirs

Pengxiang Wang, Wanying Yu, Juan Huang, Qiang Zou, Zhengtao Yang

School of Resources and Environment, Henan Polytechnic University, Henan, China

ABSTRACT

China has abundant deep coalbed methane (CBM) resources. Exploration and development efforts this year have revealed that deep CBM reservoirs are characterized by large resource volumes, intact coal structures, high gas content, high gas saturation, and significant development potential. However, significant differences in reservoir properties between deep and shallow coal seams, particularly in pore structure and fracture characteristics, pose challenges. These differences obscure gas migration patterns and make it difficult to establish effective development techniques. To address these challenges, this study examines deep coal reservoir samples from the Turpan-Hami and Junggar Basins. A comprehensive analysis of reservoir properties was conducted using multiple experimental methods. The findings reveal the multi-scale pore development and fracture characteristics of deep coal reservoirs, providing a theoretical basis for further exploration and development of deep CBM resources.

KEYWORDS

Deep coalbed methane; Reservoir properties; Pore characteristics; Fracture characteristics.

1. INTRODUCTION

As both the source and reservoir of coalbed methane (CBM), coal reservoirs play a crucial role in determining the development potential and effectiveness of CBM extraction[1]. Consequently, their physical properties have become a focal point in CBM exploration and development worldwide.Researchers generally recognize that coal reservoirs exhibit a "dual-porosity" system composed of pores and fractures[2]. The adsorption capacity, gas content, and permeability of these reservoirs are closely linked to the development and structural characteristics of these pores and fractures[3].Advances in reservoir characterization techniques and experimental methods have enabled more precise multi-scale analyses. Such studies are essential for understanding CBM occurrence, desorption-diffusion behavior, seepage capacity, and enrichment mechanisms, bridging the gap between macroscopic and microscopic characterization.Current coal reservoir characterization methods can be broadly classified into fluid-intrusion and non-fluid-intrusion techniques.The fluid-intrusion method involves injecting a non-wetting fluid (e.g., mercury) or an adsorptive gas (e.g., CO_2 or N_2) into a sample under pressure. By recording the relationship between injection volume and pressure, key pore-fracture structure parameters—such as pore size distribution (PSD), specific surface area (SSA), and pore volume (PV)—can be derived using appropriate theoretical models.Common fluid-intrusion techniques include mercury intrusion porosimetry (MIP)[4], low-temperature nitrogen adsorption (LPN_2GA)[5], and low-temperature carbon dioxide adsorption ($LPCO_2GA$)[6].Dou et al. utilized mercury intrusion experiments to analyze coal reservoir pore structures from three perspectives: pore-throat distribution, fractal characteristics, and capillary pressure patterns[7].Yao et al. compared traditional MIP with constant-rate mercury intrusion (CMP)

and concluded that CMP is a more effective method for characterizing coal pore size distribution, particularly in providing detailed macropore information[8].Mercury intrusion porosimetry is primarily suitable for characterizing mesopores and macropores[9].Under isothermal conditions, CO_2 and N_2 molecules can serve as adsorption probes to analyze coal surface and pore structure characteristics. Combining LPN_2GA with scanning electron microscopy (SEM) allows for a more detailed visualization of the pore structure in coals of varying metamorphic degrees, including pore volume, SSA, pore size distribution, and pore morphology.The low-temperature N_2/CO_2 adsorption method, a conventional pore characterization technique, preserves the integrity of the sample but requires a low-temperature environment and is unsuitable for moist samples. Furthermore, due to the kinetic diameters of N_2 (20.364 nm) and CO_2 (20.33 nm) and the resolution limitations of analytical instruments[10], this method can only identify micropores (<10 nm) and small mesopores (10–100 nm). It cannot accurately characterize larger pores, which is why researchers increasingly integrate multiple techniques for comprehensive coal structure characterization.

In summary, the integration of advanced, non-destructive testing technologies has facilitated the transition of coal reservoir characterization from qualitative to quantitative analysis.In this study, a detailed analysis of deep coal reservoir properties was conducted using advanced techniques, including nitrogen adsorption, high-pressure mercury intrusion, scanning electron microscopy, and isothermal adsorption methods.

2. EXPERIMENTS

2.1. Introduction to the Study Area

This study focuses on the deep coal reservoirs of the Turpan-Hami Basin and the Junggar Basin. The Turpan-Hami Basin, located in northwestern China, is a multi-cycle superimposed basin that developed on a Precambrian crystalline basement and a Paleozoic folded basement. The most extensive coal-bearing sedimentary strata in the Turpan-Hami Basin belong to the Jurassic system, with the primary coal-bearing formations being the Badaowan Formation and the Xishanyao Formation.The Junggar Basin, also located in northwestern China, is a large superimposed basin situated between the Yilinheibiergen, Zaire, and Qinggelidi Mountains. It developed on a pre-Carboniferous basement and has undergone multiple phases of basin formation. The Jurassic strata in the Junggar Basin are well developed, with multiple extensive coal seams in the Badaowan and Xishanyao Formations, making it a region rich in coalbed methane resources.

2.2. Sample Preparation

The coal reservoir samples for this study were obtained from deep drilling cores at depths of 3,310–3,336 m in the Turpan-Hami Basin and 2,243–2,266 m in the Junggar Basin. The core samples were collected from the Kexin and Cainan wells. After collection, the samples were sealed and preserved following the national standards GB/T 19222-2003 and GB/T 16773-2008.Large coal samples were first transported to the laboratory. Then, a hammer and a crusher were used to prepare 1–2 cm^3 coal blocks for high-pressure mercury intrusion and scanning electron microscopy, as well as 60–80 mesh coal powder for nitrogen adsorption analysis.

2.3. Experimental Procedure

2.3.1. Principle of the Nitrogen Adsorption Experiment

The low-temperature nitrogen adsorption method is used to measure pore distribution and structural characteristics in the 1–100 nm range. Since nitrogen is an inert gas, the experiment is conducted at liquid nitrogen temperature, minimizing the risk of chemical adsorption. Gas adsorption is commonly used to characterize pore regions that cannot be measured by mercury intrusion, particularly

nanoscale micropores and mesopores. The experiment is based on the principle that when gas molecules come into contact with a solid surface, some molecules are adsorbed onto the surface. Desorption occurs when the gas molecules acquire enough energy to overcome the surface potential of the adsorbent. Equilibrium is reached when the rates of adsorption and desorption are equal. At a constant temperature, the adsorption amount is a function of the relative pressure (P/P_0). The adsorption amount can be calculated using Boyle's law, and adsorption measurements at different relative pressures yield the isothermal adsorption curve. The isothermal adsorption curve is used to determine the specific surface area and pore size distribution. The low-temperature nitrogen adsorption experiment provides information on the distribution of small to mesopores. Based on the nitrogen adsorption-desorption curves and adsorption data, the DFT model is applied to obtain structural parameters such as pore volume, specific surface area, average pore diameter, and pore size distribution. The low-temperature nitrogen adsorption experiment was conducted using the TriStar II surface area analyzer in strict accordance with the Chinese National Standard GB/T 19587-2017 on the determination of specific surface area using the gas adsorption BET method. Upon completion of the experiment, structural parameters such as pore volume, specific surface area, average pore diameter, and pore size distribution were obtained by analyzing the N_2 adsorption-desorption curve using the BET and DFT models.

2.3.2. Principle of High-Pressure Mercury Intrusion Experiment

The mercury intrusion method can be used to characterize pore structures in coal reservoirs with diameters greater than 7.2 nm. It is an effective technique for analyzing pore types, distributions, and quantities. The fundamental principle of mercury intrusion porosimetry is based on the Laplace equation. Mercury, with a contact angle greater than 90°, does not spontaneously enter pores under ambient conditions. However, applying external pressure overcomes mercury's surface tension, forcing it into the pores. This establishes a functional relationship between the pressure required to fill a pore and its diameter, where the pressure needed to intrude mercury into a given pore conforms to the Laplace equation. In high-pressure mercury porosimetry for coal reservoirs, liquid mercury is injected into the sample. The smallest detectable pore size depends on the maximum working pressure, with a detection range of 7.5–75,000 nm. Since high-pressure mercury intrusion can create artificial pores, potentially affecting measurement accuracy, it is primarily used to analyze mesopores and macropores. The mercury intrusion experiment was conducted using the Auto Pore IV 9505 porosimeter, strictly following the Chinese National Standard GB/T 21650.1-2008, which specifies the mercury intrusion method for determining pore size distribution and porosity in solid materials. The experimental sample was a 1 cm^3 cube. After the experiment, the mercury intrusion and extrusion data provided by the instrument were analyzed using the Washburn equation to determine pore volume, specific surface area, average pore diameter, and pore size distribution.

2.3.3. Principle of Scanning Electron Microscopy (SEM) Experiment

A scanning electron microscope (SEM) consists of three main components: an electron beam emission module, a vacuum system, and an imaging module. The electron gun cathode emits an electron beam, which is accelerated under a high voltage and focused by condenser and objective lenses, forming a finely focused electron beam approximately 5 nm in diameter. The electron beam scans the sample surface in a raster pattern via deflection coils located above the objective lens, generating multiple electron signals. These signals are collected by detectors, amplified, and converted into voltage signals. The electron beam in the display tube also scans in a raster pattern on the fluorescent screen, synchronized with the sample surface scanning, thereby generating an image corresponding to the detected signals. In this study, the SEM experiment was conducted at the Key Laboratory of Henan Polytechnic University using a Quanta FEG 250 field emission scanning electron microscope (FE-SEM).The SEM experiment utilized the FEI Quanta 250 FEG field emission SEM. Under high vacuum mode, the instrument achieves a resolution of less than 1.0 nm (SE) at 30 kV, less than 2.5 nm (BSE) at 30 kV, and less than 3.0 nm (SE) at 1 kV.

3. ANALYSIS

This study adopts Hodot's decimal-based classification method for pores, categorizing them into ultramicropores (diameter <10 nm), micropores (10–100 nm), mesopores (100–1000 nm), macropores (1000–10,000 nm), and microfractures (diameter >10,000 nm).

3.1. Pore Structure Characteristics of Coal Reservoirs – Based on Nitrogen Adsorption Experiments

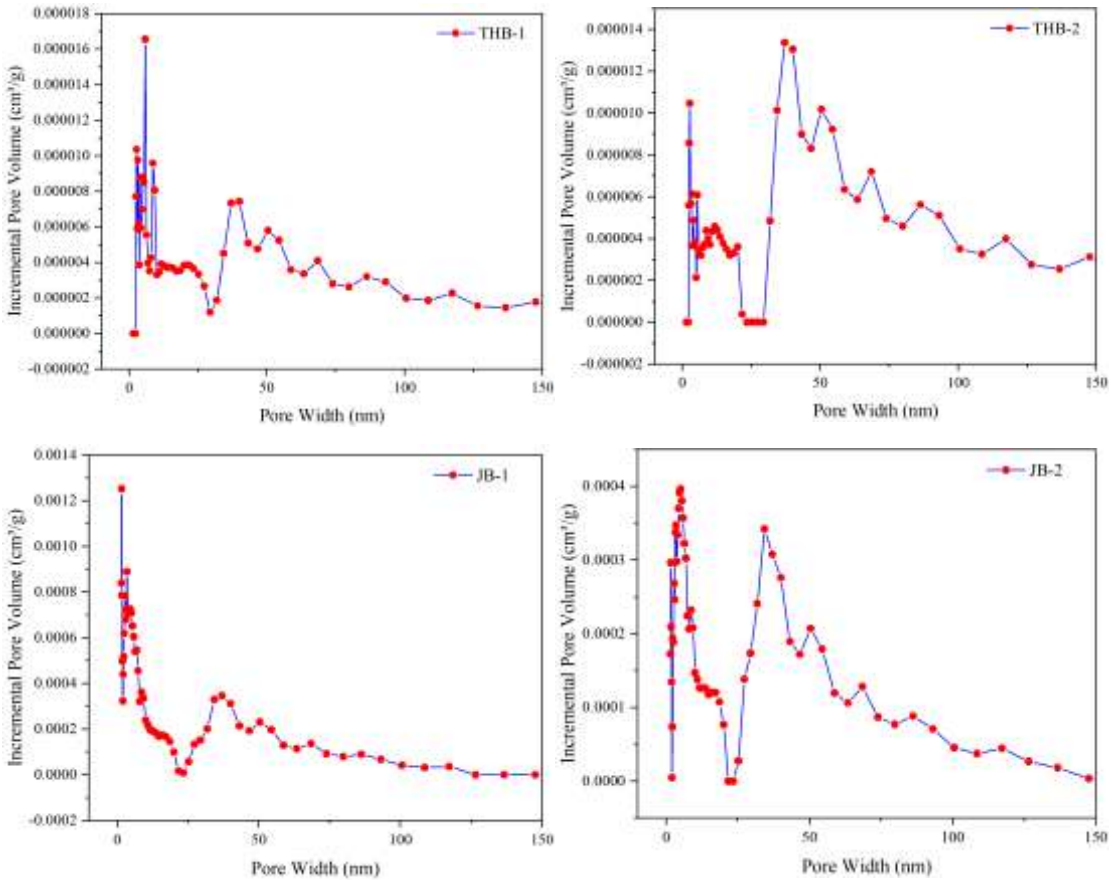

Figure 1. Pore Size Distribution Curve Obtained from Nitrogen Adsorption Experiments

The nitrogen adsorption experiment in this study utilized the Density Functional Theory (DFT) model, an effective method for describing the adsorption behavior of porous materials. The pore size distribution characteristics obtained from the DFT model are shown in Figure 1.As seen in Figure 1, the deep coal samples from the Turpan-Hami Basin exhibit significantly weaker gas adsorption capacity compared to those from the Junggar Basin. Statistical analysis shows that at 150 nm, the cumulative adsorption volume of the Turpan-Hami Basin samples ranges from 0.000261 to 0.000268 cm^3/g, whereas that of the Junggar Basin samples ranges from 0.011511 to 0.023239 cm^3/g. These results indicate that the pore development in the Turpan-Hami Basin samples is less extensive than in the Junggar Basin samples at this stage. Additionally, Figure 1 reveals that the pore development in the ultramicropore stage of the Turpan-Hami Basin samples is relatively complex, displaying a multi-peak distribution pattern. In contrast, the pore development in the Junggar Basin samples is relatively simpler, exhibiting a bimodal distribution with primary peaks at approximately 3 nm and 40 nm.

3.2. Pore Connectivity Characteristics of Coal Reservoirs – Based on High-Pressure Mercury Intrusion Hysteresis Loops

Coal pores can be classified into three types: isolated pores, connected pores, and semi-open pores. Connected pores allow gas or liquid to enter, while isolated pores remain sealed, preventing gas penetration. In high-pressure mercury intrusion experiments, pore connectivity can be analyzed based on the trends and differences observed in the mercury intrusion and extrusion curves. Previous studies have shown significant variability in coal pore development, leading to distinct differences in mercury intrusion-extrusion curves. Analyzing the hysteresis loops of these curves is an effective method for assessing pore connectivity in coal reservoir samples. The mercury intrusion-extrusion curves obtained from the experiments are shown in Figure 2. Both the Turpan-Hami Basin and Junggar Basin deep coal samples exhibit mercury hysteresis loops, but with significant differences. The hysteresis loops of the Turpan-Hami Basin samples are relatively narrow, with smaller loop areas and narrower openings. This suggests that the pores in these samples are predominantly closed or semi-closed, often exhibiting bottleneck or ink-bottle shapes, leading to poor connectivity. In contrast, the Junggar Basin samples exhibit larger and more pronounced hysteresis loops with wider openings, indicating better pore connectivity and a more uniform pore distribution compared to the Turpan-Hami Basin samples.

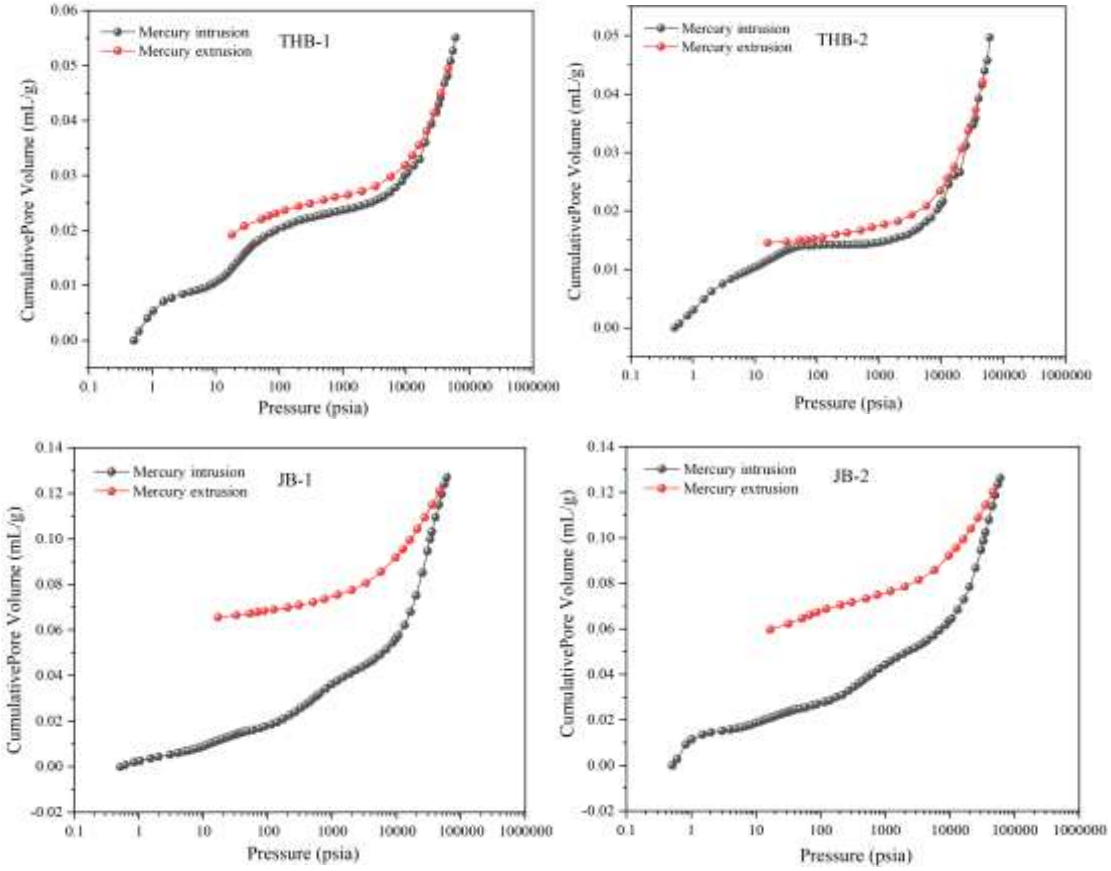

Figure 2. Mercury Intrusion and Retraction Curves Obtained from High-Pressure Mercury Intrusion Method

3.3. Multi-Scale Pore Distribution Characteristics of Coal Reservoirs Based on High-Pressure Mercury Intrusion Experiments

The pore size distribution curve obtained from high-pressure mercury intrusion experiments is shown in Figure 3. The figure presents statistical data on the distribution of micropores, small pores, mesopores, macropores, and microfractures based on the mercury intrusion results. As shown in the

figure, the pore development in deep samples from the Tuha Basin is lower than that of the Junggar Basin samples. These results are generally consistent with those obtained from nitrogen adsorption tests. In the ultramicropore stage (pore size <10 nm), the Tuha Basin samples exhibit a complex development pattern with a multi-peak distribution. In the micropore stage (10–100 nm), the Tuha Basin samples show slightly better pore development than the Junggar Basin samples, suggesting a relatively higher degree of pore formation in this range. In the mesopore stage (100–1000 nm), the Tuha Basin samples exhibit a relatively smooth distribution, whereas the Junggar Basin samples display a multi-peak distribution, indicating more extensive pore development in this range compared to the Tuha Basin samples. In the macropore stage, Sample 1 from the Tuha Basin shows relatively well-developed pores, whereas Sample 2 exhibits poorer development with a flatter curve. The Junggar Basin samples also show limited pore development in this stage. In the microfracture stage, the Tuha Basin samples demonstrate significantly better development than those from the Junggar Basin, suggesting a higher abundance of microfractures in the Tuha Basin samples.

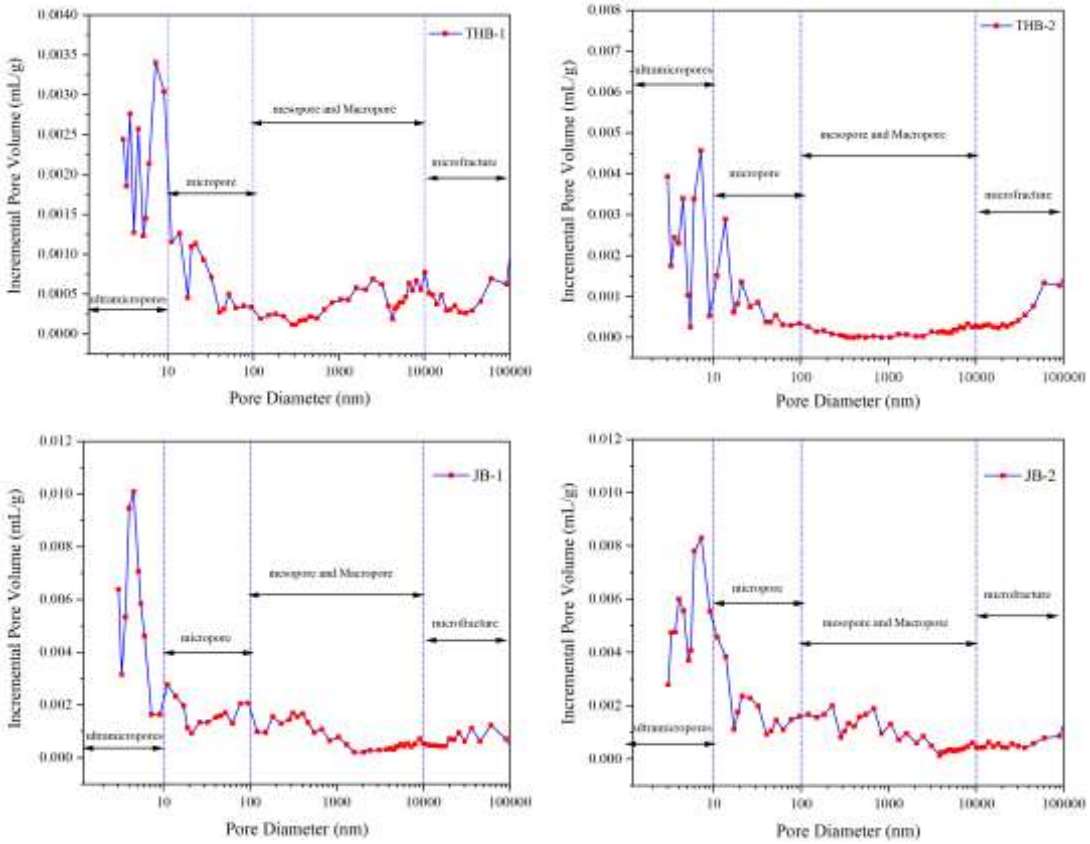

Figure 3. Pore Size Distribution Curve Obtained from High-Pressure Mercury Intrusion Method

3.4. Two-Dimensional Pore-Fracture Development Characteristics of Coal Reservoirs Based on Scanning Electron Microscopy (SEM) Experiments

The two-dimensional images obtained from scanning electron microscopy (SEM) experiments are shown in Figure 4. These images reveal that deep coal reservoir samples exhibit a diverse and complex range of pore-fracture development types. A pronounced cross-scale effect is observed in pore structures, with fractures primarily categorized as endogenous fractures, exogenous fractures, and microfractures. In Figure 4(a), the Tuha Basin sample shows a significant presence of adhered mineral deposits on its surface. A set of three intersecting fractures forming a composite fracture system is observed, characterized by narrow openings, which classify them as endogenous fractures. In Figures 4(b), (c), and (d), the Tuha Basin samples exhibit well-developed fractures, including desiccation cracks (exogenous fractures) and branched fractures (endogenous fractures). Mineral debris is frequently observed filling these fractures. In Figures 4(e), (f), (g), and (h), SEM images of

the Junggar Basin samples at 2000x magnification show well-developed microfractures and pores. Figures 4(e) and (f) display a high density of gas pores, as well as a combination of exogenous and endogenous fractures. In Figure 4(g), a well-defined T-shaped fracture is observed. The horizontal segment of the fracture remains relatively closed, while the vertical segment has a wider opening. In Figure 4(h), a distinct endogenous fracture is evident, though its openness is relatively low.

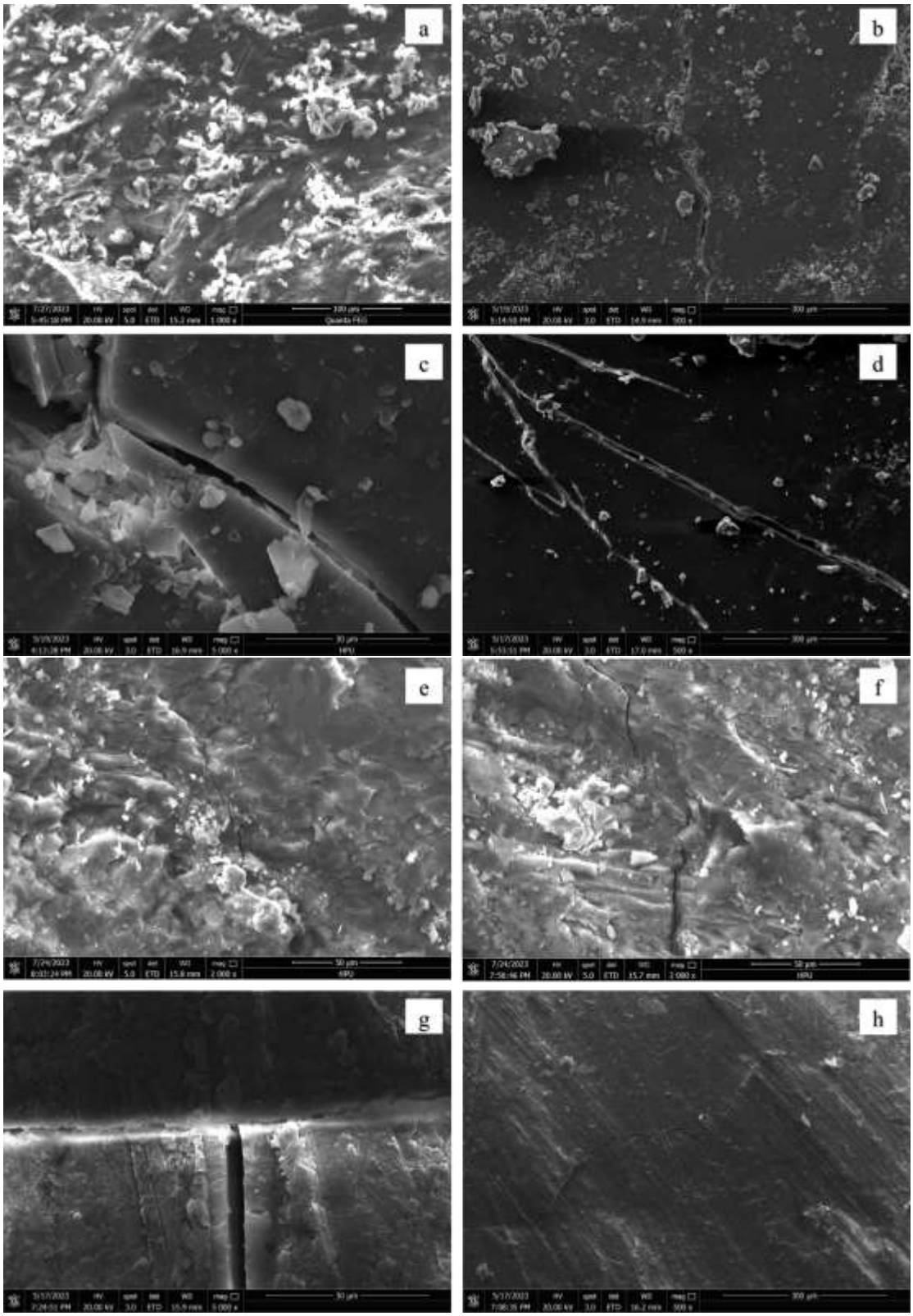

Figure 4. Sample Surface Images Obtained from Scanning Electron Microscopy (SEM) Experiments

4. CONCLUSIONS

With the development of coalbed methane (CBM) extraction, it has been found that deep coal seams are rich in CBM. However, research indicates that the reservoir properties of deep coal seams differ significantly, leading to notable variations in gas content, gas occurrence characteristics, gas saturation, preservation conditions, and drainage performance. Therefore, this study employs multiple technical methods to precisely characterize the pore-fracture development in coal reservoirs, aiming to provide theoretical support for large-scale exploration and development of deep CBM. The key findings are as follows:

(1) Nitrogen adsorption tests indicate that deep samples from the Tuha Basin have lower gas adsorption capacity than those from the Junggar Basin. The Tuha Basin samples exhibit a multi-peak pore distribution during the nitrogen adsorption stage, whereas the Junggar Basin samples predominantly show a bimodal distribution.

(2) High-pressure mercury intrusion tests provide intrusion-retrogression curves for samples from the Tuha and Junggar Basins. Analysis shows that the Tuha Basin samples contain a high proportion of closed and semi-closed pores, resulting in poor connectivity, whereas the Junggar Basin samples exhibit better pore connectivity. The multi-scale pore distribution analysis further reveals that the Tuha Basin samples have more developed pores in the small-pore and microfracture stages, while the Junggar Basin samples show superior development in the ultramicropore and mesopore stages.

(3) Scanning electron microscopy (SEM) analysis reveals well-developed pores and fractures in deep samples from both basins, with a pronounced cross-scale effect. The identified fracture types include endogenous fractures, exogenous fractures, desiccation cracks, and branched fractures. Some fractures are filled with particulate minerals, and an interwoven development of endogenous and exogenous fractures is observed.

REFERENCES

[1] Shen, C. (2023). Study on the physical characteristics of the No. 3 coal reservoir in Yuecheng Wellfield. Coal, 32(05), 17–21.

[2] Tao, S., Wang, Y., Tang, D., Xu, H., He, W., & Li, Y. (2012). Pore–fracture system of the southern coal seam in the Qingshui Basin and its contribution to permeability. Journal of College Geology, 18(03), 522–527.

[3] Yuan, Y. (2022). Study on the physical properties and enrichment regularities of the coalbed methane reservoir in the Xishanyao Formation of western Zhun Nan [Dissertation, China University of Mining and Technology (Beijing)].

[4] Jiang B, Qu Z, Wang G G X, et al. Effects of structural deformation on formation of coalbed methane reservoirs in Huaibei coalfield, China[J]. International Journal of Coal Geology, 2010,82(3-4):175-183.

[5] Schmitt M, Fernandes C P, Da Cunha Neto J A B, et al. Characterization of pore systems in seal rocks using Nitrogen Gas Adsorption combined with Mercury Injection Capillary Pressure techniques[J]. Marine and Petroleum Geology, 2013,39(1):138-149.

[6] Yu S, Bo J, Fengli L, et al. Structure and fractal characteristic of micro- and meso-pores in low, middle-rank tectonic deformed coals by CO2 and N2 adsorption[J]. Microporous and Mesoporous Materials, 2017,253:191-202.

[7] Dou, W., Liu, L., Wu, K., & Xu, Z. (2016). Study on the pore structure of low-permeability reservoirs and its influence on permeability based on mercury injection experiments: A case study of the Chang-7 reservoir of the Triassic Yanchang Formation in the southwestern Ordos Basin. Geological Review, 62(02), 502–512.

[8] Yao Y, Liu D. Comparison of low-field NMR and mercury intrusion porosimetry in characterizing pore size distributions of coals[J]. Fuel, 2012,95:152-158.

[9] Nie B, Liu X, Yang L, et al. Pore structure characterization of different rank coals using gas adsorption and scanning electron microscopy[J]. Fuel, 2015,158:908-917.

[10] Wang, C., Bao, Y., & Ju, Y. (2020). Characterization of the evolution of the microscopic pore structure in biogasified coal organic rock reservoirs using FE-SEM, HIP, and N_2 adsorption experiments. Earth Science, 45(01), 251–262.